Visual and Spectroscopic Demonstration of Intercrystalline Migration and Resultant Photochemical Reactions of Aromatic Molecules Adsorbed in Zeolites

Shuichi Hashimoto* and Junko Kiuchi

Chemistry Department and Advanced Engineering Courses, Gunma College of Technology, Maebashi, Gunma 371-8530, Japan

Received: May 1, 2003; In Final Form: June 22, 2003

We applied a fluorescence microscopy method to investigate the intercrystalline migration of aromatic molecules adsorbed in faujasite zeolites aiming at observing directly the particle-to-particle processes dependent both on interparticle distance and on the time scale of the observation. Photophysical processes such as intersystem crossing and energy transfer and photochemical reactions such as charge transfer (CT) and triplet−triplet energy transfer between guest species incorporated in the zeolites were exploited as indicator reactions to yield a luminescence color characteristic of individual zeolite particles. Two types of migration mechanisms were observed: a through-space diffusional transfer mode between separated zeolite crystals and a molecular injection process from a loaded crystal to another unloaded crystal, both in contact. A preferential direction of guest migration was found to exist for a few cases: for instance, aromatics such as phenanthrene and chrysene migrate from sodium form of zeolite X (Na^+-X) to thallium-exchanged zeolite X (Tl^+-X). On the other hand, the migration-assisted formation of CT complexes between electron-donating arenes such as phenanthrene and chrysene, and electron-accepting 1,2,4,5-tetracyanobenzene, both incorporated into separate zeolite Na^+-X crystals, takes place as a result of the migration of the donors. Comparison of this technique with a conventional fluorescence spectroscopic method for zeolite powders revealed that the microscopy method is advantageous because it is difficult for the spectroscopic method to detect the evolution of new emission bands in strongly emitting matrix. The fluorescence microscopy method utilizing photochemistry in zeolites was found to be a powerful technique for the qualitative investigation of the intercrystalline migration in zeolites.

Introduction

Diffusion in zeolites plays an important role in most of the applications of zeolites as adsorbents and catalysts.[1] A typical schematic picture of the diffusion in a group of these microporous crystals is drawn in Scheme 1 in which adsorbed species are shown to migrate among a few adsorption sites within a cage besides a jump to neighboring cages through interconnecting windows, and occasionally travel from one zeolite crystal to another.

Thus the diffusion of adsorbed species in zeolites is primarily divided into two classes, intercrystalline and intracrystalline migration, the latter being further subdivided into two categories, intracage migration and intercage jump between the neighboring cages. Within the context of intracrystalline migration, intercage hopping requires a relatively high activation barrier and, therefore, constitutes a slow process, allowing the guest molecules to move around the adsorption sites within a given cage before they can finally jump out. Various methods have been developed for the measurement of intracrysalline diffusivity of adsorbed species including the NMR spin−lattice relaxation,[2] pulsed field gradient (PFG) NMR,[3] quasielastic neutron scattering (QENS)[4] and triplet−triplet energy transfer[5] techniques. The results were also discussed on a theoretical basis utilizing molecular dynamics[6] and Monte Carlo simulation[7] methods.

In contrast, intercrystalline diffusion attracted less attention because of lack of a proper experimental methodology. The intercrystalline diffusion is complicated by adsorption, intracrystalline diffusion, and desorption processes acting as a rate-determining step and extends over a wide area of space. Thus the relaxation methods that have been successful for the measurement of intracrystalline diffusivity are not applicable because of an inappropriate time scale of the observation. For these reasons, more qualitative investigations have been reported. In one such study, Yoon's group observed the intercrystalline migration of NaI salt intercalated in zeolite Na^+-Y upon physical contact at ambient temperature with $MV^{2+}-Y$ (methyl viologen dication-exchanged Y) or $DQ^{2+}-Y$ zeolite (diquart-exchanged Y).[8] The contact-induced color change due to the formation of ion pairs, $[MV^{2+\bullet}I^-]$ (yellow) and $[DQ^{2+\bullet}I^-]$

SCHEME 1: Pictorial Representation of the Diffusion of Molecules in a Zeolite Particle[a]

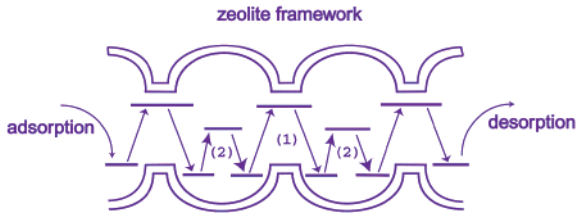

[a] The intracrystalline diffusional motion is classified as two types according to the nature of activation energy: (1) activation energy for intercage jump and (2) activation energy for intracage jump. On the other hand, intercrystalline diffusion is a sequential process of jumps from one crystal to another. The desorption and adsorption of molecules at every step are necessary for this process.

* To whom correspondence should be addressed. E-mail: hashi@chem.gunma-ct.ac.jp.

10.1021/jp035180o CCC: $25.00
Published on Web 08/12/2003

(orange), within the supercages was indicative of the migration. A narrow glass tube packed with NaI-doped Na^+-Y on the one side and $MV^{2+}-Y$ on the other side showed that the colorization takes place only in the $MV^{2+}-Y$ layer while the Na^+-Y layer remains colorless, suggesting that the NaI salt is indeed migrating. Although the study gained a certain insight into the intercrystalline transport of materials by visual representation, the experimental method seems too qualitative and macroscopic. In addition to the migration of the guest species, exchange of charge-compensating cations was demonstrated by Fyfe and co-workers to occur between different zeolite crystals through physical contact between the crystals.[9] The structural change accompanying the cation exchange between Na^+-A and Li^+-A was monitored by powder X-ray diffraction (XRD) and ^{29}Si magic angle spinning (MAS) NMR studies. The rate was found to depend on the amount of mechanical mixing, the degree of hydration, and the crystallite size. Thus semiquantitative results were presented for the cation migration.

Here we show an unprecedented approach to the observation of the intercrystalline migration of guest aromatic species in zeolites based on fluorescence microscopy. The fluorescence microscopy was successfully applied previously by Calzaferri's group to the investigation of the intercalation, alignment, and energy transfer of dye molecules in the channel-type zeolite L crystals of $1-3\ \mu$m size.[10] However, the technique has not been applied to the study of interzeolite diffusion. We have looked at individual zeolite particles of micrometer size loaded with aromatic guest molecules under a microscope to detect the migration of the molecules between the particles by luminescence color changes exploiting photophysical processes such as intersystem crossing and energy transfer assisted by charge-compensating cations, and also charge-transfer complex formation. Although still qualitative, the present results indicate clearly the migration of aromatic molecules between zeolite crystals in a micrometer to several hundred micrometer range.

It is noteworthy that Ramamurthy and co-workers previously attempted to observe the interparticle migration of aromatic molecules between two types of cation-exchanged zeolites with a luminescence spectroscopy exploiting the heavy atom effect.[11] They mixed, for example, Na^+-Y complexed with naphthalene and unloaded Cs^+-Y and followed the emission spectral change for 5 days. If naphthalene molecules migrated from Na^+-Y to Cs^+-Y, they should have seen the emission spectral change from fluorescence bands to phosphorescence bands assisted by the heavy atom perturbers in the Cs^+-Y. They reported that they did not see any change in the emission spectra, indicating that no migration of the guest from one zeolite to the other occurred at room temperature. This is probably because the fluorescence spectroscopic method is not sensitive enough to detect the evolution of a new emission band in a strongly emitting matrix when applied to the powdered samples, as we will show in this report.

Experimental Section

Sodium form of zeolites X (Na^+-X; Si/Al = 1.26, Na/Al = 1.0), Y (Na^+-Y; Si/Al = 2.75, Na/Al = 1.0), and A (Na^+-A; Si/Al = 1.0, Na/Al = 1.0), and potassium form of zeolite L (K^+-L; Si/Al = 3.0, K/Al = 0.98, Na/Al = 0.02) were obtained from Tosoh. Cation-exchanged zeolites were prepared via ion exchange of Na^+-X, Na^+-Y, and Na^+-A according to the procedure described in the literature.[11] The exchange ratio was determined by atomic absorption analysis to be 86−98% for Tl^+ exchange and 70−85% for Tb^{3+} and Eu^{3+} exchanges. Zeolite powder was calcined in air at 450 °C for 8 h just before sample preparation. Zeolite samples doped with aromatic molecules were prepared by adsorption from *n*-hexane solution: the dehydrated zeolite powder was stirred in *n*-hexane solution of each molecule in a stoppered vial at room temperature for 10 min; the sample was filtered, and the solid was washed twice with *n*-hexane. All of the procedures were carried out in a glovebox charged with N_2. The zeolite powders were transferred into a container attached to a 2-mm-thick Suprasil cell for optical measurements and evacuated at <0.4 Pa for 12 h at 100 °C.

The ground-state reflectance spectra of powdered samples were measured on a Shimazu UV-3101PC double-monochromator spectrophotometer equipped with an integrating sphere coated with $BaSO_4$. The reference was $BaSO_4$ (Kodak white reflectance standard). Absorption spectra of ground-state species were obtained by using the Kubelka−Munk function. Fluorescence spectra were recorded on a Hitachi F-3010 fluorescence spectrophotometer with front face geometry. Optical microscopy pictures of luminescent samples were obtained with 100−400 times enlargement on an Olympus BX-51-FL microscope attached to a Nikon Coolpix 5000 digital camera (5 megapixels). The excitation light emanating from a 100 W mercury lamp was passed through an appropriate excitation cube composed of an excitation filter (330−385 nm), a dichroic mirror, and a cutoff filter (cutoff wavelengths < 400 nm). Zeolite crystals, prepared by loading aromatics on dehydrated materials and kept in a container sealed under vacuum, were spread on a cover glass, which was then fixed at the peripheral part on a slide glass with Teflon shield paste to minimize the intrusion of moisture; this plate was used as a sample for the microscopy study. Pictures recorded on the digital camera were processed with an imaging software (Adobe Photoshop). The mass-spectrometric temperature-programmed desorption (TPD) data were collected on a Rigaku TPD type R machine connected to a quadrupole mass filter. Helium gas (flow rate = 100 $cm^3\ min^{-1}$) was used as a carrier gas throughout the measurements. The TPD run was carried out at a linear heating rate of 10 K min^{-1} from ca. 50 to 800 °C. About 50 mg of a zeolite sample was used in one run.

Results and Discussion

1. Probing Intracrystalline Migration with Fluorescence Spectroscopy. We first check the applicability of fluorescence spectroscopy to monitor the diffusion of aromatic species adsorbed in zeolites. We begin with presenting the results of intracrystalline diffusion. A fixed quantity of anthracene (1.3×10^{-4} mol/g), which has a short axis shorter in length than the diameter of the widows to the supercages, 0.74 nm,[12] was adsorbed on Na^+-Y zeolite by sublimation at 160 °C for 27 h in an evacuated container, followed by the measurement of the emission spectra of the samples with the evolution of time. In one experiment, a sample was allowed to stand at room temperature, while in the other, another sample was kept in a drying oven at 160 °C. Figure 1A compares the emission spectra of these samples. Initially, a broad and structureless emission band centered at 500 nm ascribable to the excimer emission is dominant, in addition to a structured band assignable to the monomer emission (Figure 1A, line 1). When kept at 160 °C for a week, the contribution of the excimer emission pronouncedly decreased (Figure 1A, line 2), indicating that the anthracene molecules initially accumulated as aggregates on the external surfaces of the zeolite particles thus giving rise to the excimer emission diffused apart into the inner surfaces of the particles, leading to the observation of the emission largely of

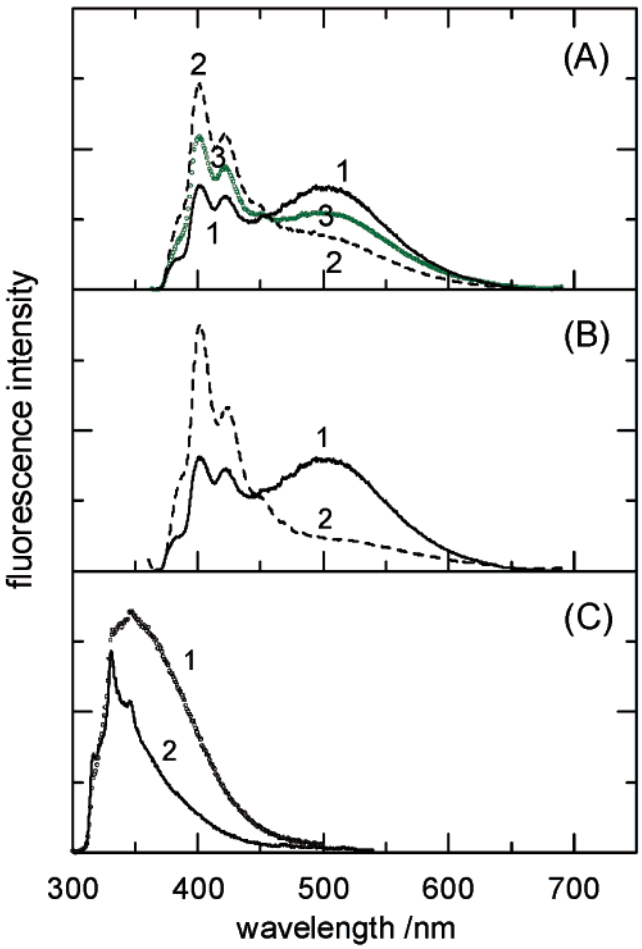

Figure 1. Emission spectra (A) of 1.3×10^{-4} mol·g^{-1} anthracene adsorbed by sublimation on Na^+-Y zeolite in a vacuum (1) measured following 27 h of heating at 160 °C after the mixing of the zeolite powders with anthracene crystals by breaking a seal, (2) measured after an additional week of heating at 160 °C, and (3) measured after the sample was kept at room temperature for 2 months following the same treatment as that of spectrum 1, (B) of 1.3×10^{-4} mol·g^{-1} anthracene adsorbed by sublimation on Na^+-Y zeolite in a vacuum (1) measured following 27 h of heating at 160 °C after the mixing of the zeolite powders with anthracene crystals by breaking a seal, (2) measured on addition of 0.10 cm^3·g^{-1} of water by breaking a vacuum seal (measured 10 min after the treatment) to the sample in spectrum 1, and (C) of naphthalene adsorbed by sublimation in a vacuum on zeolite K^+-L at ambient temperature (1) measured 24 h after the mixing of the zeolite powders with naphthalene crystals by breaking a seal and (2) measured after heating the same sample as that in spectrum 1 at 110 °C for 12 h.

the monomer. Note that these aggregates do not correspond to the microcrystals because anthracene crystals do not show the excimer emission.[13] In contrast, when kept at room temperature, the contribution of the excimer emission is reduced but still substantial even after 2 months (Figure 1A, line 3), suggesting that the diffusion of anthracene from the exterior surface to the interior of the particles is very slow at room temperature. Accordingly, by exploiting the monomer−excimer emission spectral behavior of anthracene, the fluorescence spectroscopic method can qualitatively indicate the location of molecules adsorbed on zeolites as to the inside or outside of the crystals and also track their diffusional motions driven by the concentration gradient.

When Na^+-A zeolite, which has a smaller pore entry aperture of 0.41 nm[12] than that of Na^+-Y, is employed instead of Na^+-Y for the gas-phase adsorption of anthracene, the emission spectrum from the resulting powder consists entirely of the excimer emission and does not alter the shape even after a prolonged period of heating. The result can be interpreted by the notion that anthracene molecules initially adsorbed on the exterior surface cannot diffuse into the pores because of the size exclusion by the small entry aperture, reinforcing the validity of our fluorescence spectroscopic method to monitor the molecular diffusion in zeolites.

Strikingly, the introduction of small quantity of water and other small solvent molecules (acetonitrile, methanol, pyridine, etc.) drastically accelerated the diffusion of anthracene into the inside of the Na^+-Y zeolite particles. The spectral change from the excimer to the monomer emission takes place immediately on introduction of water in a vacuum by breaking a seal, as revealed from Figure 1B. According to the previous study of decay rates for triplet-state anthracene in zeolite Na^+-Y with various degrees of hydration, the mobility of anthracene is enhanced dramatically in the presence of 0.05−0.15 cm^3/g of water.[14] A similar conclusion was drawn on the effect of coadosorbed water on the mobility of phenanthrene and naphthalene in zeolite K^+-Y from the quenching experiment of these triplet states by Ellison.[15] Thus the observation in the presence of coadsorbed water is also explained by the exterior to interior diffusion but in this case with much faster rate.

In another test of the location of luminescent probe molecules in zeolites, naphthalene adsorbed from gas phase at room temperature on zeolite K^+-L bearing one-dimensional channels of a diameter of 0.71 nm[12] was studied. Figure 1C, line 1, shows the emission spectrum of the zeolite sample in which naphthalene was sublimed in an evacuated container by allowing it to stand for 24 h at room temperature. The spectrum is attributed to the emission bands of naphthalene monomer superimposed on a broad and featureless emission band ascribable to the second excimer that assumes partially overlapped geometry of the naphthalene moieties.[16] The contribution of the emission due to the second excimer reduced greatly on heating the sample at 100 °C for 12 h as shown in Figure 1C, line 2, and thus the broadness depends on the amount of the molecules adsorbed on the exterior surfaces of the zeolites as aggregates, suggesting that the emission spectrum assignable to the second excimer at relatively low loadings is a good indication of the adsorption of naphthalene on the outer surfaces. Notably, benzophenone can also act as an active probe molecule to indicate location in zeolites because it is nonphosphorescencent on the outer surfaces presumably because of self-quenching caused by the formation of aggregates but phosphoresces at room temperature when located inside the cages and channels.

Overall, these results show that the intracrystalline motion of guest molecules from the exterior to the interior of the zeolite crystal can be monitored qualitatively using a few luminescent probe molecules. This might be useful for the assessment of the nature of adsorption sites and the diffusional motion of these molecules within the zeolite crystals. We now scrutinize the applicability of the fluorescence spectroscopy to monitor the intercrystalline migration of aromatic species.

2. Intercrystalline Migration of Guest Molecules and Resultant Photochemical Reactions. *A. Fluorescence Spectroscopic Observation of Zeolite Powders.* The charge-balancing cations are largely responsible for the adsorption of benzene and other aromatic species within zeolite cavities and channels.[17] During the course of our research on photochemistry of aromatic molecules adsorbed in zeolites,[18] we noted that preferential adsorption takes place for a zeolite crystal with particular cations over another zeolite with a different kind of cations. For instance,

circumstantial evidence suggests that zeolite Tl^+-Y has much stronger affinity for aromatic molecules than Na^+-Y has. Here, we employ phenanthrene (Phe) as a luminescencent probe molecule instead of anthracene used in section 1. The advantage of Phe over anthracene is that Phe adsorbed in zeolites always gives only the monomer emission spectrum and shows no loading-dependent behavior, which has been observed for anthracene. The emission spectra of phenanthrene (Phe) adsorbed from *n*-hexane solution into mixed powders (1:1 in weight) of Na^+-Y and Tl^+-Y exhibited mostly phosphorescence at room temperature, which implies that Phe molecules are mostly adsorbed in Tl^+-Y, even in the presence of Na^+-Y. Note that in Tl^+-exchanged zeolites phosphorescence emission has been almost exclusively observed for many aromatic molecules because of the enhancement of spin−orbit coupling by the action of Tl^+ ions while only fluorescence can be observed in zeolite Na^+-Y at room temperature.[11] The result prompted us to investigate the preference of a type of zeolite particle over another by the adsorbed species.

Zeolite Na^+-Y powder incorporated with Phe was mixed with unloaded zeolite Tl^+-Y powder in an evacuated container, and the time evolution of the emission spectra of the sample was studied. To facilitate the diffusion of Phe, the sample was heated in a drying oven at 100 °C. Just after the mixing of the powders, only the fluorescence bands of Phe were recorded, analogous observation to that of Phe adsorbed in Na^+-Y; however, on heating the sample for a certain period, the evolution of the phosphorescence bands of Phe was detected, the contribution of which increases at the expense of that of the fluorescence bands with the heating time, Figure 2a. The evolution of the phosphorescence arises either from the migration of Phe from the Na^+-Y powders to the Tl^+-Y powders or from the migration of Tl^+ ions from the empty Tl^+-Y powders to the Na^+-Y zeolites incorporating Phe. The cation exchange has been demonstrated between Na^+-A and Li^+-A previously.[9] To determine which of the species actually migrates, another experiment was carried out using a sample of Phe/Na^+-Y mixed with unloaded zeolite Tl^+-A instead of Tl^+-Y (Figure 2b). Zeolite Tl^+-A, in principle, can incorporate no Phe into its cavities (α-cages) because the entry aperture size (0.41 nm[12]) of the α-cages is smaller than the dimension of the short axis of Phe. We have evidence that the maximum loading level of Phe on Na^+-A was estimated to approximately 100 times less than that of Phe in Na^+-Y by the measurement of adsorption isotherm. This is also the case for Tl^+-A.

Close scrutiny of Figure 2a in comparison with Figure 2b reveals that the migration of Tl^+ does take place to some extent but more importantly that Phe migrates from Na^+-Y to Tl^+-Y zeolite crystals, judging from appreciably larger spectral changes observed in Figure 2a. We will confirm the same conclusion by means of fluorescence microscopy in the next section, but in the meantime, we will proceed to detect the intercrystalline migration and resultant chemical reactions to check the applicability and limitation of the conventional fluorescence spectroscopic method.

Importantly, the monodirectional migration of Phe molecules can be postulated to take place from the Na^+-Y powders to the Tl^+-Y powders because we failed to observe the emission spectral changes in a sample of Phe/Tl^+-Y powders mixed with unloaded Na^+-Y powders when the measurements were carried out after heating at 100 °C for more than 20 h. The concept of the monodirectional migration is also applicable to naphthalene (Nap) from Tb^{3+}-exchanged zeolite Y ($Tb^{3+}-Y$) to zeolite Na^+-Y as depicted in Figure 3. The excitation of Nap

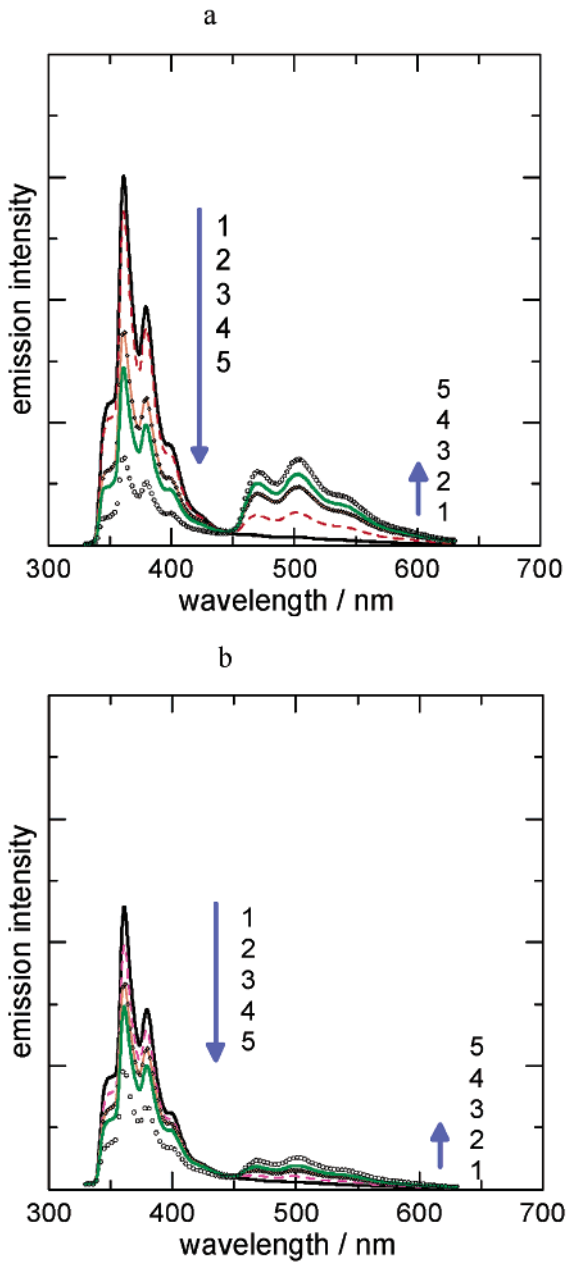

Figure 2. Emission spectral changes (λ_{ex} = 320 nm) of mixed powders of zeolite Na^+-Y (0.25 g) incorporated with 5.0×10^{-5} mol·g^{-1} phenanthrene (Phe) and (a) unloaded Tl^+-Y (0.30 g) or (b) × unloaded Tl^+-A (0.30 g) on heating at 100 °C at various times of delay: (1) 0 h; (2) 1 h; (3) 3 h; (4) 6 h, (5) 15 h.

incorporated in $Tb^{3+}-Y$ gives rise to the enhanced emission from Tb^{3+} ions due to intrazeolite energy transfer;[19b] however, when the sample of Nap/$Tb^{3+}-Y$ mixed with unloaded Na^+-Y is kept at 100 °C for 2 h, an increased fluorescence intensity of Nap was observed at the expense of the emission of Tb^{3+} ions (see Figure 3B), suggesting that Nap migrates from $Tb^{3+}-Y$ to Na^+-Y. In contrast, the migration in the reverse direction does not take place, as shown in Figure 3A.

The driving force of the guest migration in zeolites is generally ascribed to the gradient of the chemical potential.[20] The intracrystalline migration of molecules takes place from the exterior surfaces to the open interior parts of the zeolite crystal. In a similar manner, the intercrystalline migration should take place from crystals loaded with molecules to the unloaded ones although for the diffusion to take place there exists no

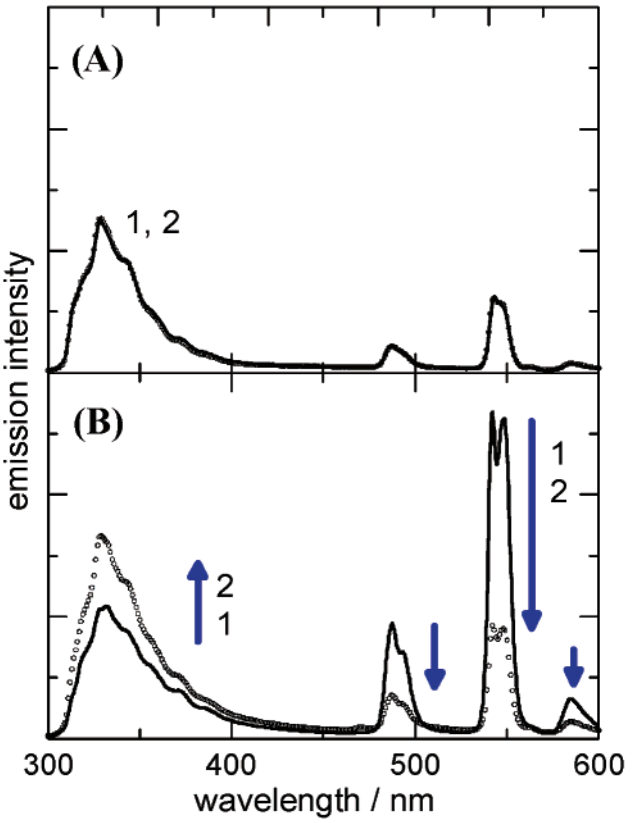

Figure 3. Emission spectral changes ($\lambda_{ex} = 280$ nm) of mixed powders of zeolite Na^+-Y (0.25 g) and $Tb^{3+}-Y$ (0.30 g), one of which is incorporated with Nap, on heating at 100 °C: (A) Nap/Na^+-Y + unloaded $Tb^{3+}-Y$ after (1) 0 h and (2) 10 h; (B) Nap/$Tb^{3+}-Y$ + unloaded Na^+-Y after (1) 0 h and (2) 10 h. An emission band at 300−400 nm is ascribed to the fluorescence of Nap, while three sharp bands from 480 to 600 nm are due to the emission of Tb^{3+} ($^5D_4 \rightarrow {}^7F_J$, $J = 6, 5, 4$). The excitation at 280 nm brings about both the emission of Nap fluorescence and that of Tb^{3+} luminescence in $Tb^{3+}-Y$. However, if Nap is incorporated in $Tb^{3+}-Y$, enhanced emission of Tb^{3+} luminescence can be observed because of the energy transfer from Nap, which does not take place for Na^+-Y incorporating Nap.

preference to particular zeolite crystals. However, if the diffusion takes place under the influence of external drifts such as electrostatic and dispersion forces between the host zeolite and guest species, the monodirectional migration can be observed between the two types of zeolite crystals with differing affinity.[21] We assume that the values of the activation energy for adsorption of guest species from one zeolite crystal to another can constitute a good measure to explain the different affinity of Phe to Na^+-Y from that of Phe to Tl^+-Y and also to predict the direction of the migration. Nevertheless, a conventional method for evaluating such an activation energy is unavailable for us at this moment. Therefore, we estimate qualitatively the adsorption energy of Phe both in Na^+-Y and Tl^+-Y zeolites by a thermal desorption method with mass-spectrometric detection. Figure 4a,b compares the thermal desorption (TPD) curve of Phe in Tl^+-Y with that of Phe in Na^+-Y.

In Figure 4, the abscissa represents the temperature of the samples and the ordinate represents the ion yields of desorbed species, along with their fragments. The mass-spectrometric scrutiny at various temperature reveals that bands appearing from 100 to 200 °C are attributable to ions originating from adsorbed water (not shown) and *n*-hexane, a solvent used for the adsorption of Phe, whereas bands occurring from 500 to 700 °C are assignable to Phe ($m/e = 178$) and its fragments. Most importantly, the peak temperature of the Phe molecular

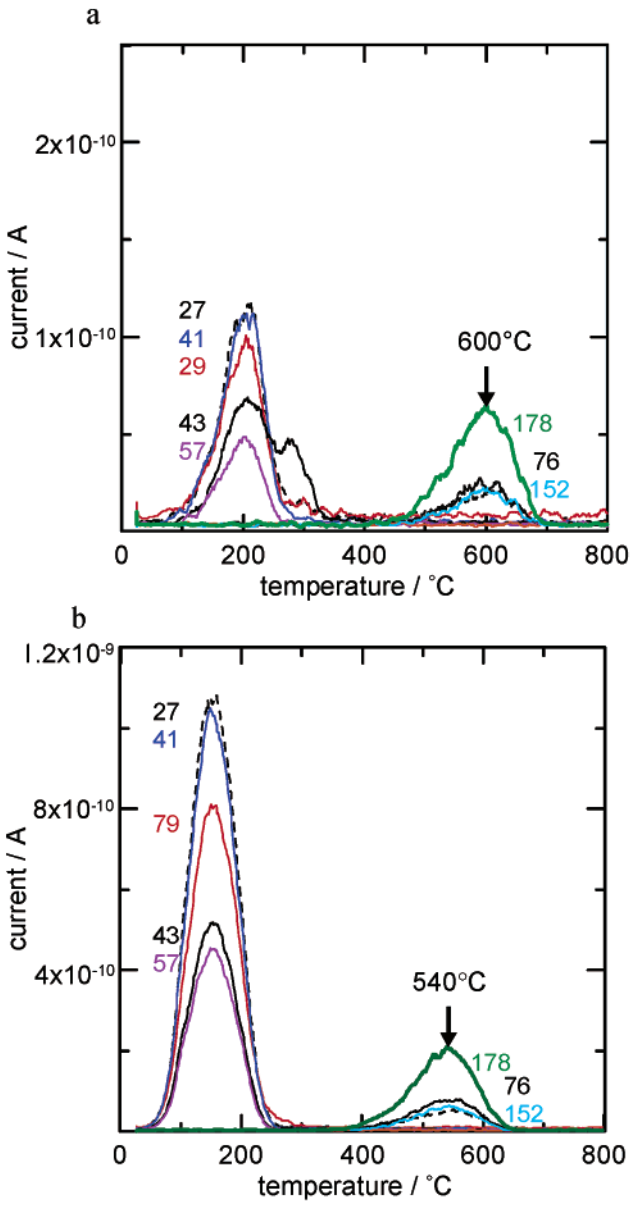

Figure 4. Temperature-programmed desorption (TPD) curves of Phe adsorbed in (a) Tl^+-Y and (b) Na^+-Y. Each curve represents the desorbed species and their fragments measured with a mass-spectrometric method at a given temperature. The number associated with each curve indicates the *m/e* of detected ions; for instance, 178 means Phe molecular ions.

ion (M^+) band in Tl^+-Y, 600 °C, is definitely higher than that of the M^+ band in Na^+-Y, 540 °C, suggesting that Phe molecules are, on average, more tightly adsorbed in Tl^+-Y. Obviously, this deduction is consistent with the observed direction of migration of Phe from Na^+-Y to Tl^+-Y. However, the temperature range in which Phe molecules desorb in the TPD measurements is surprisingly higher than the range in which the migration of Phe was detected by the emission spectroscopic measurements. Thus, the present TPD result may only qualitatively account for the stability of adsorbed species in zeolites with different cations. For more satisfactory explanation of the direction of the migration, quantitative estimation of the activation energy of adsorption is necessary; such a project is currently underway by the measurement of TPD curves as a function of heating rates.

Now we investigate the possibility of the occurrence of chemical reactions resulting from intercrystalline migration; one

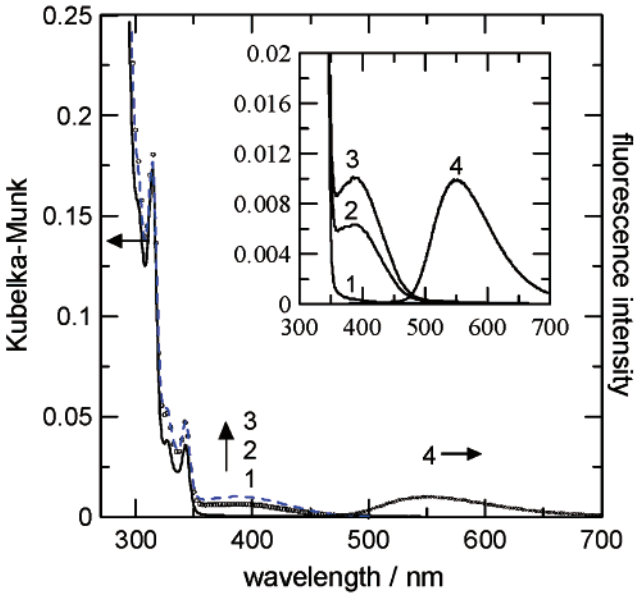

Figure 5. Absorption (Kubelka−Munk remittance function) and emission spectra of 1:1 ratio-mixed powders of zeolite Na^+−Y incorporating 5.0×10^{-5} mol·g^{-1} Phe and that incorporating 5.0×10^{-5} mol·g^{-1} TCNB. Time-dependent changes in the absorption spectra due to the formation of CT absorption band on heating at 100 °C are shown: (1) absorption at 0 h; (2) absorption at 1 h; (3) absorption at 2 h; (4) emission at 2 h. The inset shows a magnified view of the CT absorption and emission spectra.

of the successful examples is the formation of charge transfer (CT) complexes. Previously, the intrazeolite formation of the CT complexes was demonstrated by the observation of distinctive CT absorption bands between guest arene donors externally introduced and pyridinium acceptors such as methyl viologen dication incorporated into the zeolites via ion exchange with the charge-compensating cations.[22] Later, our group showed that CT complexes between the neutral guest species, electron-donating aromatics, and electron-accepting 1,2,4,5-tetracyanobenzene (TCNB) formed within zeolite cavities can be detected by the CT fluorescence bands, as well as by the CT absorption bands.[23] These observations were made by incorporating the donor and acceptors into the cavities of one zeolite crystal. Here, to further investigate the intercrystalline migration through CT formation, we prepared mixed powders consisting of donor Phe/Na^+−Y and acceptor TCNB/Na^+−Y. The absorption spectral changes were followed on heating the sample at 100 °C, as shown in Figure 5. Initially no absorption band attributable to Phe and TCNB CT complexes is present because the donor and acceptor molecules are adsorbed on the separated crystals; however, on heating the sample, the CT absorption band evolved and intensified with time. Moreover, an emission band ascribable to the CT fluorescence was observed on excitation of the CT absorption band. Both of these observations are indicative of intercrystalline migration-assisted CT complexation because the absorption and emission bands observed are quite similar to those of the Na^+−Y zeolite crystals incorporated simultaneously with Phe and TCNB.[23]

The present results show that the intercrystalline migration of aromatic species is observable by means of a conventional fluorescence spectroscopy if a proper system is chosen. The heating of the samples was a prerequisite for facilitating the migration of these species. The major drawback of the method is that the heating for a prolonged period causes the exchange of the charge-compensating cations between the zeolite crystals

SCHEME 2: Pictorial Representation of Three Types of Intercrystalline Migration Modes Assumed in the Present Study

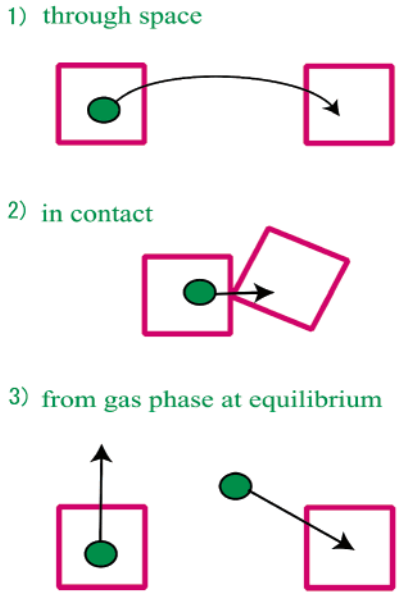

besides the guest migration. The necessity of the prolonged heating is basically due to the low sensitivity of the method to detect minor emission spectral changes buried in a strongly emitting surrounding environment. Another important drawback of this spectroscopic investigation of the powders is that the method cannot give a detailed picture of the event. For instance, we cannot tell which of the molecules, Phe or TCNB or both, moves in the migration-assisted CT complex formation and how far the molecules migrate at a given condition. We show in the following section that the fluorescence microscopy investigation is advantageous for such detailed investigations.

B. Fluorescence Microscopy Observation of Zeolite Particles. Here we apply fluorescence microscopy to the study of intercrystalline migration of aromatic molecules adsorbed in zeolites to observe directly particle-to-particle processes dependent both on interparticle distance and on the time scale of observation. The microscopy observation was made in the atmosphere at ambient temperature. As was demonstrated in the previous section, the use of zeolites for emission studies is advantageous because the observation of room-temperature phosphorescence, as well as fluorescence, from guest aromatic molecules can be made without great difficulty.[18] Besides, by exciting guest species, sensitized emission of the host zeolite is available for particular charge-compensating cations such as Eu^{3+} and Tb^{3+}.[19] One disadvantage is that a prolonged exposure, ca. >5−6 h, to the atmosphere brings about significant hydration of the host zeolites. Under fully hydrated conditions, plain aromatic molecules such as anthracene adsorbed in the cavities are eventually squeezed out and crystallize outside of the zeolite crystals;[24] therefore, it is preferable to carry out the experiments within 2−3 h. We employed X-type zeolites for the microscopy study instead of Y-type used in the fluorescence spectroscopic investigation simply because of the conveniently larger crystal size of the zeolite X (2−3 μm) as compared to zeolite Y (<1 μm). Because both zeolites, X and Y, belong to the same crystal structure of faujasite (FAU) and only differ in Si/Al ratio,[12] we assume that there is not much difference in the two zeolites for the present investigation.

We assume three types of interparticle migration modes as depicted in Scheme 2. First, molecules may jump from one

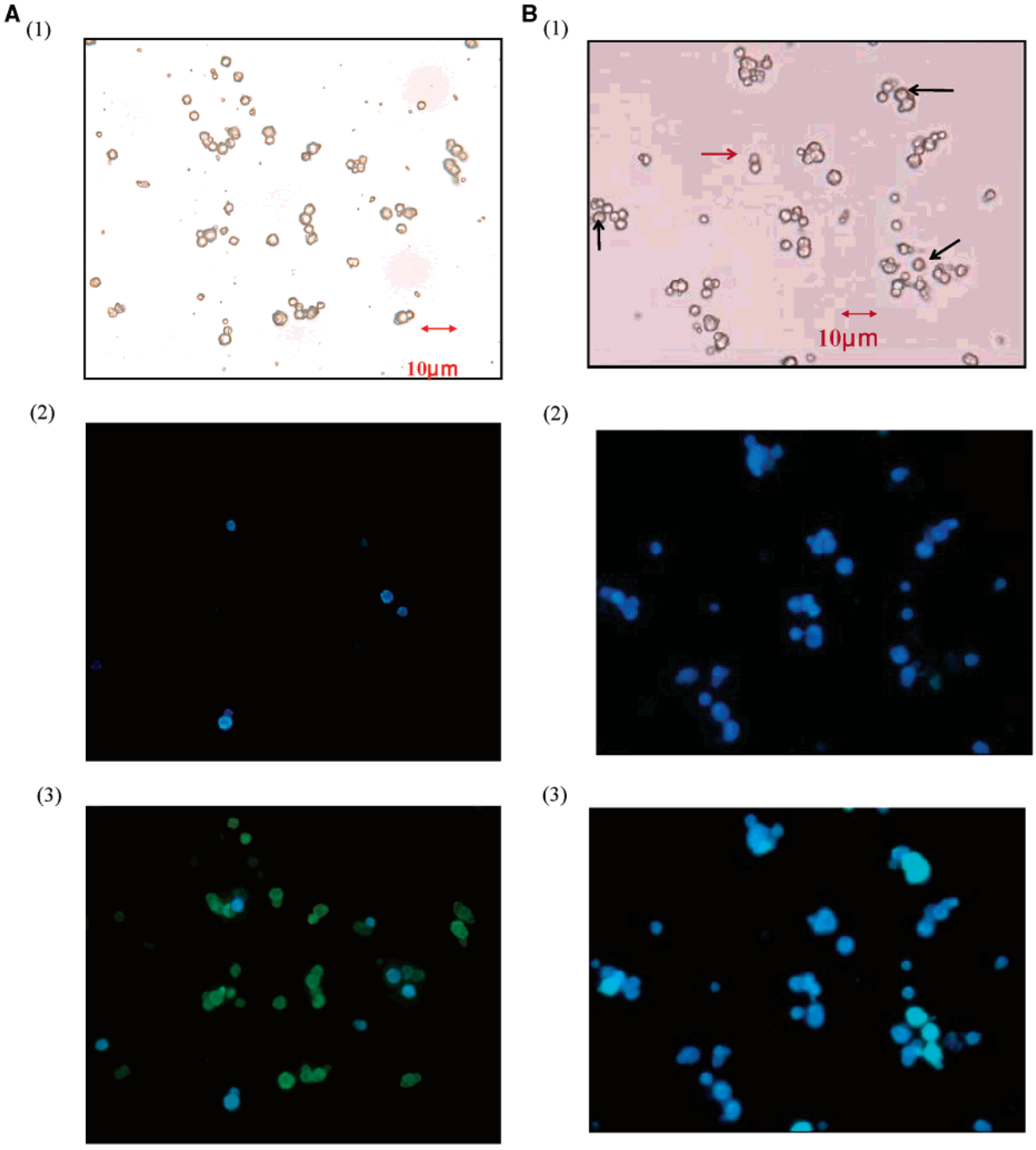

Figure 6. Optical (transmittance) and fluorescence microscopic images (400 times magnification) of zeolite Na^+-X crystals incorporating 5.0×10^{-5} mol·g^{-1} Phe mixed with unloaded zeolite Tl^+-X crystals. The same location in the sample is shown in pictures 1, 2, and 3: (A1) transmittance microscopic picture; (A2) fluorescence microscopic picture just after the sample preparation; (A3) fluorescence microscopic picture after heating the sample for 1 h at 120 °C; × (B1) transmittance microscopy picture; (B2) fluorescence microscopy picture just after the sample preparation; (B3) fluorescence microscopic picture after heating the sample for 1 h at 80 °C. In panel B, particles indicated by the arrow are the zeolite Tl^+-X: particles indicated by the black arrow show the change from nonemissive to green-emissive because of a close contact with the blue emissive Phe/Na^+-X particles, and a particle indicated by the red arrow shows no change due to a distance from the blue emissive particles.

zeolite crystal to another (case 1) depending on the distance, temperature, and pressure. The values of diffusion coefficient (D) for aromatics in air may give an idea of the average diffusion distance ($\sqrt{\langle r^2 \rangle}$) dependent on the time (t) required for the diffusion as[7a]

$$\sqrt{\langle r^2 \rangle} = \sqrt{6Dt} \qquad (1)$$

provided that molecules are desorbed form the zeolites. The value of D for benzene is known to be 9.6×10^{-6} m^2 s^{-1} at 298 K in air,[25] but it is not known for the other molecules such as Nap and Phe. For benzene, we predict from eq 1 the value of $\sqrt{\langle r^2 \rangle}$ to be 7.6 μm, 240 μm, 7.6 mm, and 0.50 m at $t = 1$ μs, 1 ms, 1 s, and 1 h, respectively. Thus, for benzene analogues, the microscopic investigation of the intercrystalline diffusion should be possible because the migration distance is expected to be within the range of observation. The second interparticle migration mode (case 2 in Scheme 2) is possible when the zeolite crystals are actually in physical contact. This type of migration has the advantage of requiring only a small or negligible amount of desorption energy. Finally in the third mode, if the vapor pressure of the molecules is such that

equilibrium is established between molecules adsorbed and those in the gas phase, exchange between the gas phase and the adsorbed species should take place. This, in effect, leads to the migration from one zeolite to another (case 3). With this in mind, we carried out the experiments described next.

Figure 6A shows optical (transmittance) and fluorescence microscopy pictures of a sample in which zeolite Na^+-X crystals incorporating Phe (Phe/Na^+-X) are mixed with unloaded Tl^+-X zeolite crystals. The pictures were recorded for the sample just after the mixing and after 2 h of heating at 120 °C. The transmittance microscopy pictures were recorded to show the location of the zeolite particles, both emissive and nonemissive. The pictures also confirm that the particles themselves do not relocate their positions during and after the heating. The fluorescence microscopy picture just after the mixing shows that only the Phe/Na^+-X particles emit blue fluorescence of Phe, while the unloaded Tl^+-X particles are nonemissive. On heating the sample, the Tl^+-X particles (originally nonemissive) emit green phosphorescence of Phe, suggesting unequivocally that the migration of Phe molecules takes place from the Na^+-X to the Tl^+-X particles. The present observation is basically the diffusional migration of Phe between the zeolite particles because the observation of the migration of Phe from Na^+-X to unloaded Na^+-X crystals was made with the fluorescence microscopy method on heating at 100 °C. However, we failed to observe the migration of Phe from Tl^+-X to unloaded Na^+-X crystals, reinforcing the validity of the conclusion of the monodirectional migration process from the Na^+-X to the Tl^+-X, obtained in the fluorescence spectroscopic study of powders in the preceding section.

Notably, the migration of Phe is considered to take place by the through-space and in-contact mechanisms. We cannot distinguish the mechanisms, case 1 and case 3, because of the prolonged heating time, which far exceeds the time scale of diffusion of Phe over the distances in observation, such as 10−100 μm. The major difference in the cases 1 and 3 is that the former requires a desorption process with relatively high activation energy, while the latter requires negligibly small activation energy for desorption. We also found that mild heating restricts the migration of Phe only to the Tl^+-X crystals located in close proximity of the Na^+-X particles (Figure 6B).

The observation of a larger area with low magnification is instructive. For such an example, we give chrysene (Chry)/Na^+-X and unloaded Tl^+-X mixed system as depicted in Figure 7. In Figure 7, not only the migration of Chry from the Na^+-X area to the Tl^+-X area but also the migration of Tl^+ from the Tl^+-X area to the Na^+-X area was observed to take place. The migration of Tl^+ ions appears to proceed through space without the physical contact of crystals; however, the detail of the mechanism is yet to be investigated. One possibility is that water vapor, which can move freely from one crystal to another, is responsible for the cation migration by forming clusters containing the cations.

As a prototypical example of fluorescence microscopy observation of photochemical reactions resulting from intercrystalline migration, we examined CT complexes and triplet−triplet (T−T) energy transfer. Figure 8 depicts the fluorescence microscopy pictures of TCNB/Na^+-X (A), Phe/Na^+-X (B) and TCNB/Na^+-X mixed with Phe/Na^+-X (C).

We can observe microscopically the blue fluorescence of Phe but not the fluorescence of TCNB, which occurs well below 400 nm. Surprisingly, the green CT fluorescence occurs just after the mixing of both particles at room temperature even without the contact of the zeolite particles (Figure 8C), which

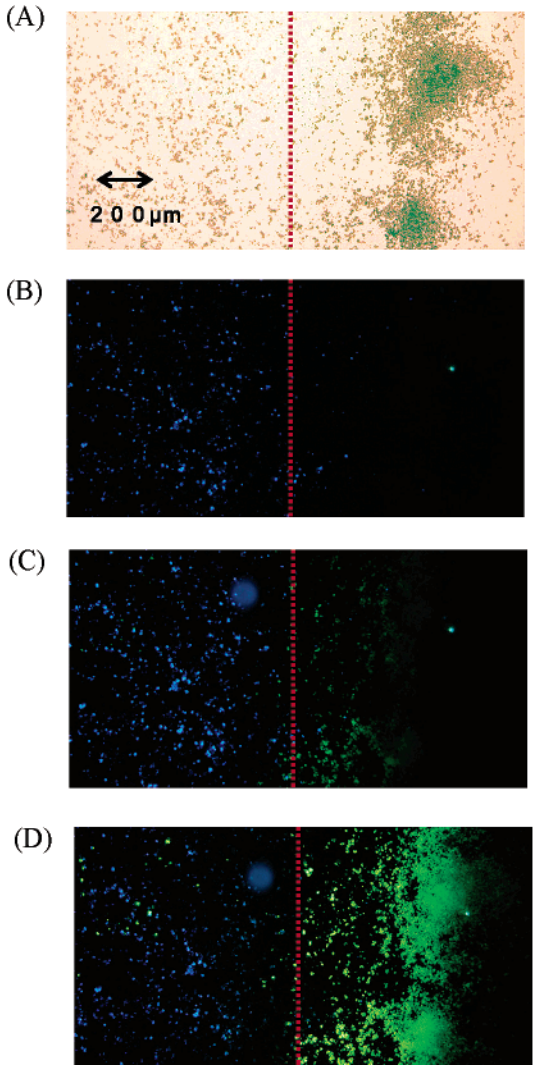

Figure 7. Optical (transmittance) and fluorescence microscopy images (100 times magnification) of zeolite Na^+-X crystals incorporating 1.0×10^{-5} mol·g^{-1} chrysene (Chry) and unloaded zeolite Tl^+-X crystals. The Chry/Na^+-X crystals are on the left side and the empty Tl^+-X crystals are on the right side: (A) transmittance image showing the distribution of the zeolite particles; (B) fluorescence image just after the preparation (only the left side gives blue fluorescence); (C) fluorescence image after being kept at 100 °C for 15 min (green emission is visible in the area near red line on the right side); (D) fluorescence image after heating at 100 °C for 25 min (green emitting area extends to the entire area on the right side and green emitting spots appeared on the left side).

was not the case when Phe/Na^+-X and Tl^+-X particles were mixed. This result suggests the importance of a driving force such as the CT interaction of guest molecules for the intercrystalline migration. However, again we cannot determine whether it is Phe or TCNB (or both) that migrates. To overcome this difficulty, we employed the less-mobile Chry instead of Phe and looked at much larger area with lower magnification. Figure 9 shows the transmittance and fluorescence microscopy pictures in such a system consisting of Chry/Na^+-X and TCNB/Na^+-X. In this case, the powders are not mixed but instead separated about 800 μm as shown in Figure 9A. Just after the sample preparation, only blue fluorescence of Chry is observable; however, after being kept at 80 °C for 10 min, green emitting particles have shown up only in the TCNB/Na^+-X side, which clearly indicates the migration of Chry taking place over a distance longer than 800 μm. This example shows the great

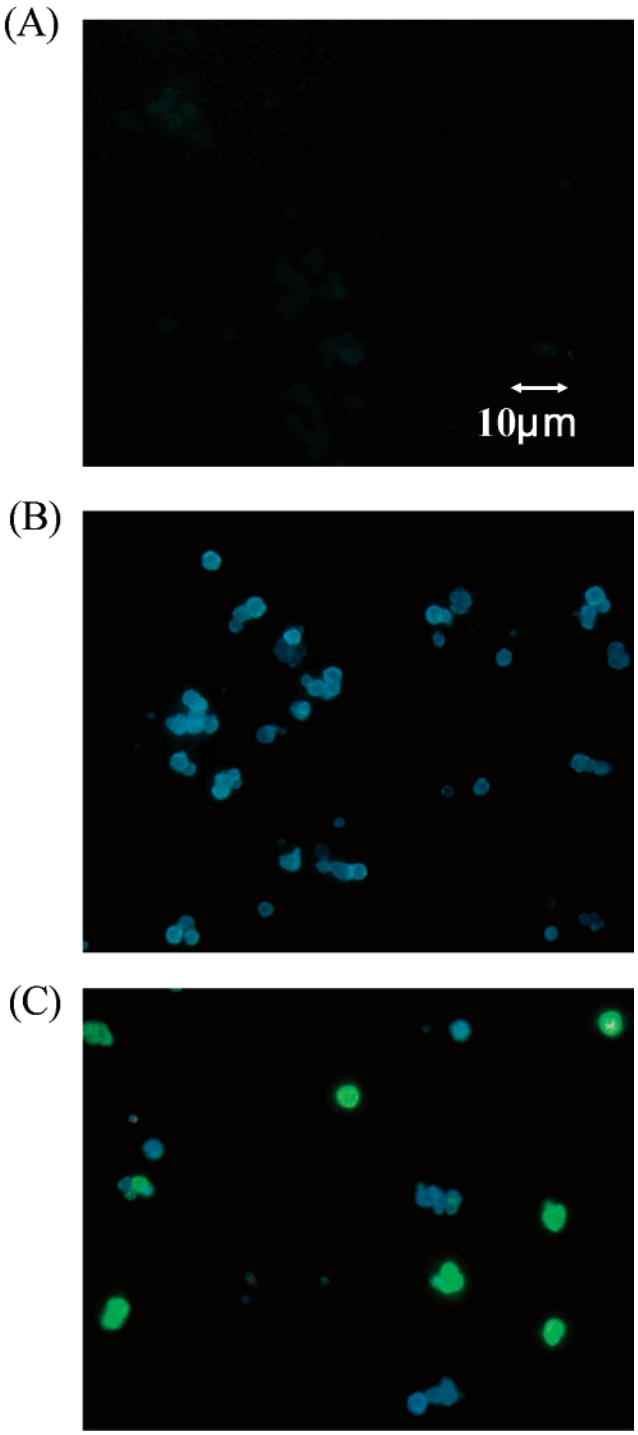

Figure 8. Fluorescence microscopy images (400 times magnification) of CT complex formation of 1,2,4,5-tetracyanobenzene (TCNB) and Phe revealing the intercrystalline migration of guest species: (A) the fluorescence image of Na^+-X crystals incorporating 3.0×10^{-5} mol·g^{-1} TCNB (no emission is observable except for the negligible contribution of the tail of the spectrum because it occurs in the UV region; (B) the fluorescence image of Na^+-X crystals (blue-emitting particles) incorporating 5.0×10^{-5} mol·g^{-1} Phe; (C) the fluorescence image of the mixed particles of TCNB/Na^+-X and Phe/Na^+-X (green-emitting particles newly appear just after the mixing while the blue-emitting particles are also present).

advantage of the microscopy method to detect which of the molecules actually moves and how far.

The second example is the triplet−triplet energy transfer between Nap and benzophenone (Bzp), a system that has been well investigated in solution and other media.[26] We employed

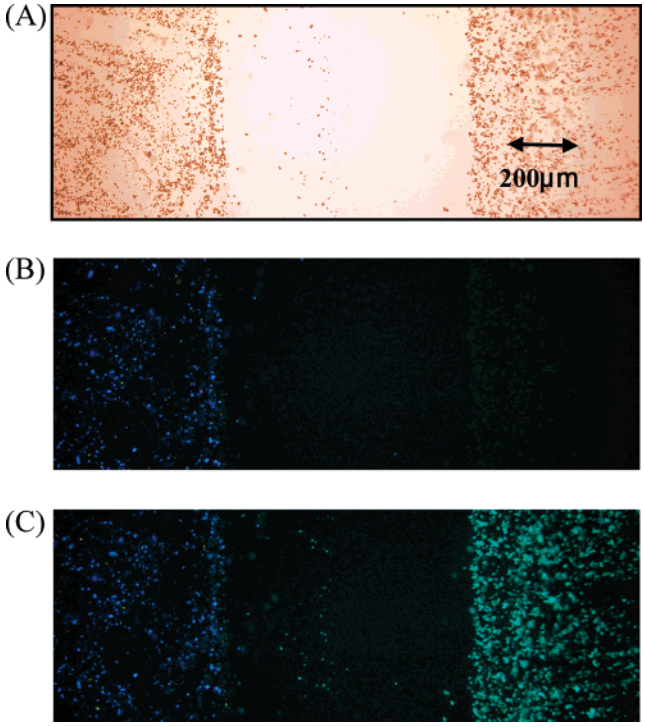

Figure 9. Microscopy images (100 times magnification) of CT complex formation of TCNB and Chry revealing the migration of Chry over several hundred micrometers: (A) transmittance microscopy image of Na^+-X crystals incorporating 3.0×10^{-5} mol·g^{-1} TCNB on the left side, Na^+-X crystals incorporating 1.0×10^{-5} mol·g^{-1} Chry on the right side, and a vacant (not strictly) area in the middle; (B) fluorescence image just after the preparation of the sample (blue fluorescence is observed only in the region on the left side); (C) fluorescence image after being kept at 80 °C for 10 min (green fluorescence is seen in the area on the right side showing the migration of Chry taking place from the left to the right).

Bzp/$Eu^{3+}-X$ and Nap/Na^+-X mixed particles for the observation, as shown in Figure 10. Note that, in Bzp/$Eu^{3+}-X$ particles, the excitation of Bzp gives rise to instantaneous energy transfer to Eu^{3+} ions in the host zeolites, leading to the observation of red emission from Eu^{3+}. Thus, just after the mixing of the powders, only red emission can be detected. However, after being kept at 100 °C for 60 min, the sample of Bzp/$Eu^{3+}-X$ and Nap/Na^+-X mixed system gives blue emission ascribable to the phosphorescence of Nap, but the sample of the Bzp/$Eu^{3+}-X$ and unloaded Na^+-X mixed system prepared for comparison purpose does not. The observation clearly indicates the occurrence of Bzp migration from the $Eu^{3+}-X$ to the Na^+-X particles. In the present system, we failed to observe this phenomenon by using the fluorescence spectrophotometer, which is most likely due to a lack of sensitivity.

Summary

The fluorescence microscopy study allowed the visual demonstration of intercrystalline migration of guest aromatic molecules incorporated into zeolites as originating from two types of mechanisms: the diffusion of the molecules through space and the molecular injection between the zeolite particles in physical contact. Photochemical processes such as charge transfer (CT) and triplet−triplet energy transfer resulting from the migration were revealed to take place for a few prototypical systems. When the migration takes place not as a simple diffusional process due to a substantial driving force, a preferential direction of the transport can be observed. The present microscopy approach is advantageous over the conven-

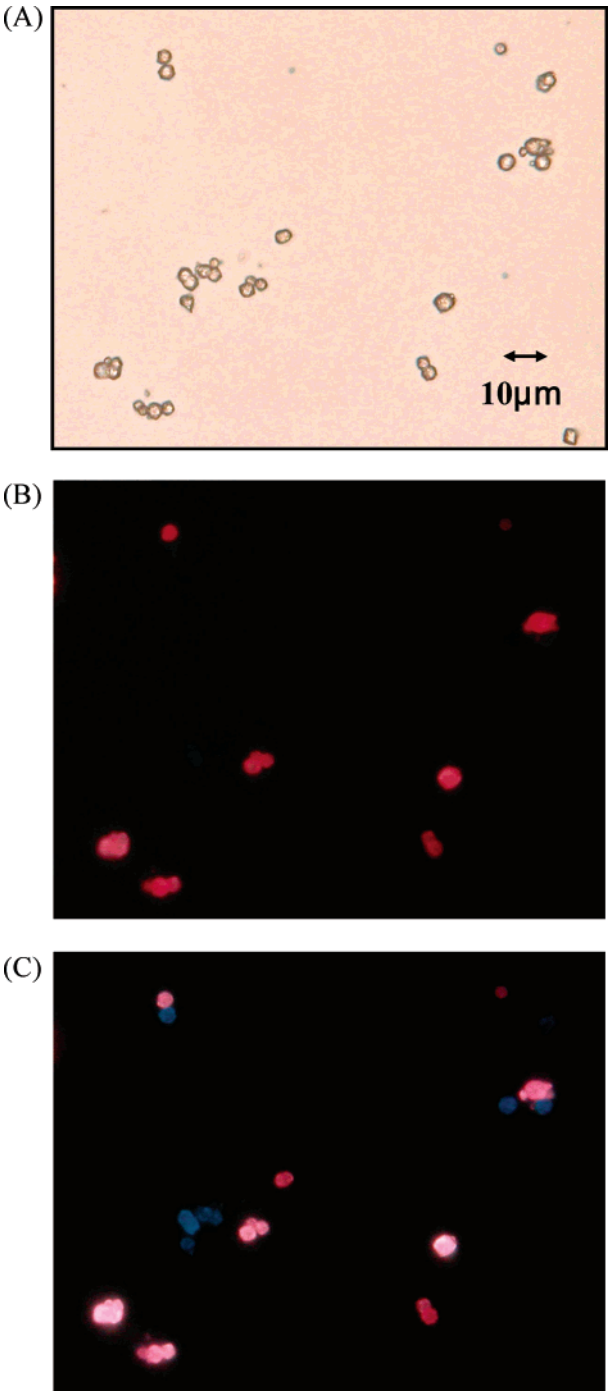

Figure 10. Microscopy images (400 times magnification) showing the evolution of blue emission from triplet-state Nap formed by the intraparticle triplet−triplet energy transfer from benzophenone (Bzp) accommodated in the same particle as a result of intercrystalline migration: (A) transmittance microscopy image; (B) fluorescence image just after the mixing; (C) fluorescence image after heating the sample for 60 min at 100 °C. Note that the emission of red color originates form zeolite Eu^{3+}−X on excitation of incorporated Bzp resulting from energy transfer to Eu^{3+} ions. Powders of 5.0×10^{-5} mol·g^{-1} Bzp/Eu^{3+}−X were mixed with those of 2.0×10^{-4} mol·g^{-1} Nap/Na^{+}−X.

tional fluorescence spectroscopic technique in terms of sensitivity for detecting minor changes in the nature of emission caused by the migration from one type of zeolite particle to another and because visualization permits the determination of the direction of migration. Thus, the fluorescence microscopy method was found to be a powerful technique for the qualitative investigation of intercrystalline migration in zeolites. For quantitative investigation, this technique should be combined with other techniques that enable the measurement of migration rate dependent on micrometer-scale distance.

Acknowledgment. This work was supported by a Grant-in-Aid for Scientific Research on Priority Areas (417, No. 15033274) from the Ministry of Education, Culture, Sports, Science and Technology (MEXT) of the Japanese Government and a Grant-in-Aid for Scientific Research (No. 14550796) from the Japan Society for the Promotion of Science. The technical assistance of Miss Yoshimi Takemoto of Gunma College of Technology and Dr. Tadashi Arii of Rigaku Co. is gratefully acknowledged. We are grateful to Professors H. Masuhara of Osaka University and T. W. Ebbesen of Louis Pasteur University for stimulating discussion and encouragement.

References and Notes

(1) (a) Kärger, J.; Ruthven, D. M. *Diffusion in Zeolites and Other Microporous Solids*; Wiley-Interscience: New York, 1992. (b) Chen, N. Y.; Degnan, T. F.; Smith C. M. *Molecular Transport and Reaction in Zeolites*; VCH: New York, 1994.

(2) (a) Burmeister, R.; Schwarz, H.; Boddenberg, B. *Ber. Bunsen-Ges. Phys. Chem.* **1989**, *93*, 1309−1313. (b) Bull, L. M.; Henson, N. J.; Cheetham, A. K.; Newsam, J. M.; Heyes, S. J. *J. Phys. Chem.* **1993**, *97*, 11776−11780. (c) Sousa Gonçalves, J. A.; Portsmouth, R. L.; Alexander, P.; Gladden, L. F. *J. Phys. Chem.* **1995**, *99*, 3317−3325. (d) Auerbach, S. M.; Bull, L. M.; Henson, N. J.; Metiu, H. I.; Cheetham, A. K. *J. Phys. Chem.* **1996**, *100*, 5923−5930.

(3) (a) Germanus, A.; Kärger, J.; Pfeifer, H.; Samulevic, N. N.; Zd'anov, S. P. *Zeolites* **1985**, *5*, 91−95. (b) Kärger, J.; Pfeifer, H. *Zeolites* **1987**, *7*, 90−107.

(4) (a) Czjzek, M.; Jobic, H.; Bee, M. *J. Chem. Soc., Faraday Trans. 1* **1991**, *87*, 3455−3459. (b) Jobic, H.; Fitch, A. N.; Combet, J. *J. Phys. Chem. B* **2000**, *104*, 8491−8497.

(5) (a) Barzykin, A. V.; Hashimoto, S. *J. Chem. Phys.* **2000**, *113*, 2841−2845. (b) Hashimoto, S.; Hagiri, M.; Barzykin, A. *J. Phys. Chem. B* **2002**, *106*, 844−852.

(6) Klein, H.; Fuess, H.; Schrimpf, G. *J. Phys. Chem.* **1996**, *100*, 11101−11112.

(7) (a) Auerbach, S. M.; Metiu, H. I. *J. Chem. Phys.* **1996**, *105*, 3753−3760. (b) Auerbach, S. M.; Metiu, H. I. *J. Chem. Phys.* **1997**, *106*, 2893−2904.

(8) Yoon, K. B.; Park, Y. S. J. *Chem. Soc., Chem. Commun*. **1993**, 522−523.

(9) Fyfe, C. A.; Kokotailo, G. T.; Graham, J. D.; Browning, C.; Gobbi, G. C.; Hyland, M.; Kennedy, G. J.; DeSchutter, C. T. *J. Am. Chem. Soc*. **1986**, *108*, 522−523.

(10) (a) Gfeller, N.; Megelski, S.; Calzaferri, G. *J. Phys. Chem. B* **1998**, *102*, 2433−2436. (b) Megelski, S.; Lieb, A.; Pauchard, M.; Drechsler, A.; Glaus, S.; Debus, C.; Meixner, A. J.; Calzaferri, G. *J. Phys. Chem. B* **2001**, *105*, 25−35. (c) Pauchard, M.; Huber, S.; Meallet-Renault, R.; Maas, H.; Pansu, R.; Calzaferri, G. *Angew. Chem., Int. Ed*. **2001**, *40*, 2839−2842.

(11) Ramamurthy, V.; Casper, J. V.; Eaton, D. F.; Kuo, E. W.; Corbin, D. R. *J. Am. Chem. Soc*. **1992**, *114*, 3882−3892.

(12) Breck, D. W. *Zeolite Molecular Sieves*; Wiley: New York, 1973.

(13) Horiguchi, R.; Iwasaki, N.; Maruyama, Y. *J. Phys. Chem*. **1987**, *91*, 5135−5139.

(14) Hashimoto, S.; Miyashita, T.; Hagiri, M. *J. Phys. Chem. B* **1999**, *103*, 9149−9155.

(15) Ellison, E. H. *J. Phys. Chem. B* **1999**, *103*, 9314−9320.

(16) Itagaki, H.; Obukata, N.; Horie, K.; Mita, I. *J. Am. Chem. Soc*. **1982**, *104*, 4469−4477.

(17) Ramamurthy, V.; Robbins, R. J.; Thomas, K. J.; Lakshiminarasimhan, P. H. In *Organized Molecular Assemblies in the Solid State*; Whitesell, J. K., Ed.; Wiley: Chichester, U.K., 1999; pp 63−140.

(18) (a) Hashimoto, S. *Solid State and Surface Photochemistry*; Ramamurthy, V., Schanze, K. S., Eds.; Marcel Dekker: New York, 2000; pp 253−294. (b) Hashimoto, S. *J. Photochem. Photobiol., C: Photochem. Rev*. **2003**, *4*, 19−49.

(19) (a) Alvaro, M.; Fornes, V.; Garcia, S.; Garcia, H.; Scaiano, J. C. *J. Phys. Chem. B* **1998**, *102*, 8744−8750. (b) Hashimoto, S.; Kirikae, S.; Tobita, S. *Phys. Chem. Chem. Phys*. **2002**, *4*, 5856−5862.

(20) Ruthven, D. M.; Post, M. F. M. In *Introduction to Zeolite Science and Practice*; Bekkum, H. V., Flanigen, E. M., Jacobs, P. A., Jansen, J. C., Eds.; Elsevier: Amsterdam, 2001; pp 525−577.

(21) Berg, H. C. *Random Walk in Biology*; Princeton University Press: Princeton, NJ, 1983.

(22) (a) Yoon, K. B. *Chem. Rev.* **1993**, *93*, 321−339. (b) Yoon, K. B. In *Solid State and Surface Photochemistry*; Ramamurthy, V.; Schanze, K. S., Eds.; Marcel Dekker: New York, 2000; pp 143−251. (c) Yoon, K. B. In *Handbook of Zeolite Science and Technology*; Auerbach, M., Carrado, K. A., Dutta, P. K., Eds.; Marcel Dekker: New York, 2003; pp 591−720.

(23) (a) Hashimoto, S.; Hagiwara, N.; Asahi, T.; Masuhara, H. *Langmuir* **1999**, *15*, 3123−3133. (b) Hashimoto, S. *Tetrahedron* **2000**, *56*, 6957−6963.

(24) Hashimoto, S.; Ikuta, S.; Asahi, T.; Masuhara, H. *Langmuir* **1998**, *14*, 4284−4291.

(25) Cussler, E. L. *Diffusion: Mass Transfer in Fluid Systems*, 2nd ed.; Cambridge University Press: New York, 1997; p 102.

(26) Turro, N. J. *Modern Molecular Photochemistry*; Benjamin: Menlo Park, CA, 1978; p 328.